Unexpected Molecular Weight Effect in Polymer Nanocomposites

Shiwang Cheng,[1] Adam P. Holt,[2] Huiqun Wang,[3] Fei Fan,[3] Vera Bocharova,[1] Halie Martin,[3] Thusitha Etampawala,[3] B. Tyler White,[1] Tomonori Saito,[1] Nam-Goo Kang,[3] Mark D. Dadmun,[3] Jimmy W. Mays,[3] and Alexei P. Sokolov[1,2,3,*]

[1]*Chemical Sciences Division, Oak Ridge National Laboratory, Oak Ridge, Tennessee 37831, USA*

[2]*Department of Physics and Astronomy, University of Tennessee, Knoxville, Tennessee 37996, USA*

[3]*Department of Chemistry, University of Tennessee, Knoxville, Tennessee 37996, USA*

(Received 4 November 2015; published 22 January 2016)

The properties of the interfacial layer between the polymer matrix and nanoparticles largely determine the macroscopic properties of polymer nanocomposites (PNCs). Although the static thickness of the interfacial layer was found to increase with the molecular weight (MW), the influence of MW on segmental relaxation and the glass transition in this layer remains to be explored. In this Letter, we show an unexpected MW dependence of the interfacial properties in PNC with attractive polymer-nanoparticle interactions: the thickness of the interfacial layer with hindered segmental relaxation decreases as MW increases, in sharp contrast to theoretical predictions. Further analyses reveal a reduction in mass density of the interfacial layer with increasing MW, which can elucidate these unexpected dynamic effects. Our observations call for a significant revision of the current understandings of PNCs and suggest interesting ways to tailor their properties.

DOI: 10.1103/PhysRevLett.116.038302

Polymer nanocomposites (PNCs) are attractive materials for many current and future technologies due to their unique ability to tune specific properties such as mechanical, thermal, optical, and even molecular and ion transport [1–5]. For example, the glass transition temperature (T_g) and zero shear viscosity of PNCs were reported to change dramatically upon adding less than 1 volume percent (vol %) nanoparticle (NP), and has been largely attributed to the changes in polymer dynamics within the interfacial region between the polymer and NP [6,7].

Because of attractive interactions, polymer chains physically adsorb to the NP's surface and form an "adsorbed bound layer" with a series of loops, trains, and tails [8–12], which has an average thickness proportional to the polymer radius of gyration (R_g) [8,13]. These adsorbed chains form a dynamic interfacial layer (DIL), which has distinct segmental mobility and other properties [7,14–23], and is believed to directly correlate with many advanced macroscopic properties of PNCs [3,5]. However, despite the recent intensive discussions on the features of the DIL [18,19,22–28], many of its characteristics, especially the basic relationship between the interfacial layer chain packing and the dynamics, are still missing. This strongly hinders our understanding of various phenomena in PNCs.

Recently, Koga *et al.* [20,29] explained the observed interfacial slowing down in supported thin films in terms of a bound loop layer (BLL) made of the loops of the adsorbed chains. According to them [20,29], the average height of the BLL provides a good estimate for the thickness of the DIL that experiences slower dynamics. Considering the analogy between polymer thin films and PNCs [7,30], it is reasonable to anticipate a similar interfacial chain packing-dynamics relationship in PNCs [31,32]. Earlier theoretical studies have shown that the average height of the BLL increases with R_g of the adsorbed polymer [8–12], and is also found to correlate well with the thickness of the DIL [18]. Thus, one should be able to tune the DIL thickness and the macroscopic properties of PNCs by a proper choice of polymer MW, providing a way to rationally design PNCs.

To verify this hypothesis, we performed detailed studies on model PNCs [15,21] using small angle x-ray scattering (SAXS), broadband dielectric spectroscopy (BDS), temperature modulated differential scanning calorimetry (TMDSC), and mass density measurements. Details of the measurements are presented in the Supplemental Material [33]. We used five different poly(vinyl acetate)s (PVAc): 12.2 kg/mol (polydispersity PDI = 1.26), 24.2 kg/mol (PDI = 1.42), 40 kg/mol (PDI = 1.76), 84.6 kg/mol (PDI = 1.79), and 253 kg/mol (PDI = 1.92) and two monodisperse poly(2-vinylpyridine)s (P2VP): 100 kg/mol (PDI = 1.07) and 400 kg/mol (PDI = 1.09). SiO_2 nanoparticles with a radius of $R_{NP} = 12.5$ nm were dispersed in polymer matrix with a fixed loadings up to $\varphi_{NP} \sim 20$ vol %. By assuming a uniform nanoparticle dispersion [16,23], an interparticle surface-to-surface distance, $d_{IPS} = R_{NP}\{[3\varphi_{NP}/(4\pi)]^{-1/3} - 2\}$, can be estimated to be ~10 nm. This distance will be slightly smaller than that in the case of assuming a random dispersion [40]. Detailed sample characterizations are presented in Table S1. We use the following definition to name our PNCs samples: Polymer MW-vol %. For example, PVAc12K-20% means a PVAc based PNC with the MW of 12.2 kg/mol and loading $\varphi_{NP} = 20$ vol%. Good dispersions of NPs are

 © 2016 American Physical Society

confirmed by the transmission electron microscopy (TEM) and SAXS as shown in the Supplemental Material [33].

Adding silica nanoparticles to PVAc leads to several changes in the dielectric spectra (Fig. 1) [15,21–23]: (i) the α-relaxation peak (segmental dynamics) shifts slightly to lower frequencies, broadens, and decreases in amplitude; (ii) an additional contribution appears on the low-frequency side (α' peak); (iii) the Maxwell-Wagner-Sillar (MWS) polarization process appears at even lower frequencies; and (iv) the conductivity changes. The α' process, corresponding to the segmental dynamics in the interfacial layer [21,23], which was not resolved in previous studies [15,21–23], is now clearly visible especially in the derivative spectra, $\varepsilon'_{\rm der}(\omega) = -(\pi/2)\partial\varepsilon'(\omega)/\partial\ln(\omega)$ (Fig. S2 in the Supplemental Material [33]), and the relaxation time distribution analysis [Fig. 1(b)] (for details of this analysis see Ref. [41] and the Supplemental Material [33]). To the best of our knowledge, this is the first clear demonstration of the interfacial layer dynamics as a well-resolved relaxation process in PNCs.

The dielectric spectra of PNCs are often analyzed as the summation of the Havriliak-Negami functions (HN fitting) of the bulk segmental peak (α peak) and of the interfacial peak (α' peak) [21,23] as shown in Fig. 1(a). We recently realized this approach ignores the heterogeneous nature of nanocomposites and is not accurate [41]. In this study, we follow a more accurate heterogeneous model approach (HMA) (see the Supplemental Material [33] and Ref. [41]).

With the clear signature of the interfacial dynamics, we analyze now the MW dependence. As shown in Fig. 2, a comparison of the samples at similar loadings reveals an unexpected effect: the increase of the MW from 12.2 to 253 kg/mol leads to a monotonic decrease in the change in segmental dynamics with a clear weakening of the α' process [Figs. 2(a)–2(b)]. The same trend can also be observed in TMDSC measurements, where the specific heat is analyzed as [23]:$C_p^{\rm mat} = (C_p^{\rm PNC} - C_p^{\rm NP} m_{\rm NP})/m_{\rm mat}$, where $C_p^{\rm mat}$,$C_p^{\rm PNC}$, and $C_p^{\rm NP}$ are the specific heat of the matrix, the PNC and the NP; $m_{\rm NP}$ and $m_{\rm mat}$ are the mass fractions of the NP and the matrix. As shown in Fig. 2(c), an increase in MW leads to a smaller shift in T_g and a weaker broadening of the glass transition step [23,25]. This trend is observed for all five MWs studied here (although only 3 representative MWs are shown in Fig. 2). Detailed analyses (Fig. S5) also show that all the dipoles relax within our frequency windows, indicating no "dead" layer in all our samples regardless of MW.

Moreover, a quantitative analysis of the BDS spectra by the HMA reveals that an increase in MW from 12.2 to 253 kg/mol leads to a change of the interfacial layer volume fraction, $\varphi_{\rm int}$, from ~25% to ~15%, corresponding to a reduction in the average interfacial layer thickness, $l_{\rm int} = \{[(\varphi_{\rm int} + \varphi_{\rm NP})/\varphi_{\rm NP}]^{1/3} - 1\}R_{\rm NP}$, from 4.1 to 2.5 nm [Fig. 3(a)]. The slowing down of the interfacial layer segmental dynamics relative to the bulk, $\tau_{\alpha'}/\tau_{\alpha}$, decreases from ~33 to ~5 [Fig. 3(b)]. The same trend is obtained using the traditional HN-fitting approach. Thus, these results are independent of the analysis and are clearly observable in the original experimental data [Figs. 2(a)–2(b)]. Furthermore, the relaxation time distribution analysis [inset Fig. 3(b)] provides the same finding: a decrease of the interfacial dynamic contribution with increasing MW. We note the relatively high polydispersity of PVAc samples caused

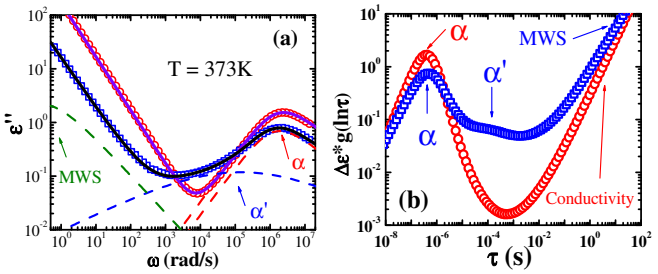

FIG. 1. (a) Comparison of dielectric loss spectra of neat PVAc40K (red circles) and PVAc40K-20% (blue squares) at T = 373 K. The dashed lines are the fits to Havriliak-Negami functions for the α process (dashed-red), α' process (dashed-blue), and the Maxwell-Wagner-Sillar polarization process (dashed-green). Solid lines present the total fit. (b) Relaxation time distribution for neat PVAc40K (red circles) and PVAc40K-20% (blue squares), where the α' process can be clearly identified.

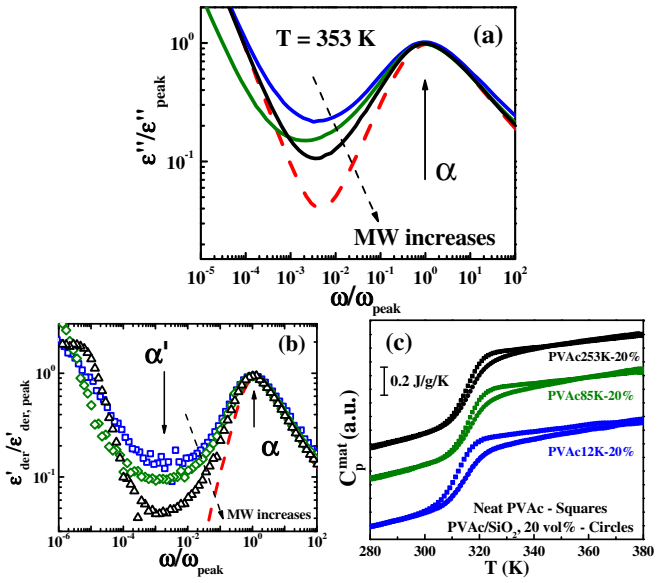

FIG. 2. Normalized dielectric loss spectra $\varepsilon''(\omega)$ (a) and derivative spectra $\varepsilon'_{\rm der}(\omega)$ (b) of PNCs with 3 selected MWs in comparison to the neat polymer PVAc85K spectrum at T = 353 K. The spectra of the α process in the studied neat polymers are identical, regardless of MW. (a) and (b) The dashed-red line, neat PVAc85K; blue line or squares, PVAc12K-20%; green line or diamonds, PVAc85K-20%; black line or triangles, PVAc253K-20%. (c) TMDSC of different PNCs and neat polymers. The y axis is arbitrarily shifted for clarity.

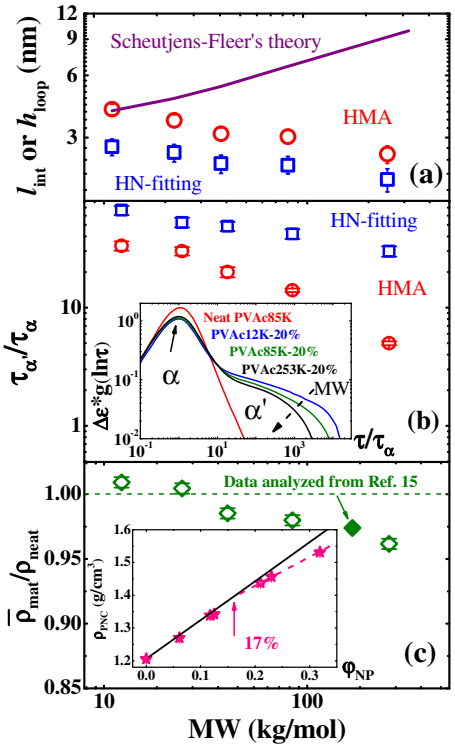

FIG. 3. (a) The estimated l_{int} by HMA (red circles) and HN fittings (blue squares). The h_{loop} is calculated by SFT with different MWs. (b) The average interfacial slowing down, $\tau_{\alpha'}/\tau_{\alpha}$, for different MWs estimated from both the HMA and the HN fitting at T = 353 K. The inset shows the relaxation time distribution spectra of α and α' for different PNCs, where the dashed arrow indicates an increase in MW. (c) The relative average density of the matrix, $\bar{\rho}_{\mathrm{mat}}/\rho_{\mathrm{neat}}$, for different PNCs at T = 293 K. The filled diamond is reanalyzed data from Ref. [15] on PVAc167K-28.2% at 293 K and 10 MPa. The inset presents the mass density (error bars are within the symbols) of PVAc40K/SiO_2 PNCs with different loadings up to $\varphi_{\mathrm{NP}} = 31.9\%$. The black line is a prediction of the two phase mixing rule: $\rho_{\mathrm{PNC}} = \rho_{\mathrm{NP}}\varphi_{\mathrm{NP}} + \rho^{\mathrm{neat}}_{\mathrm{PVAc}}(1-\varphi_{\mathrm{NP}})$. A deviation occurs at ~17 vol%, where $d_{\mathrm{IPS}} \sim 12$ nm is about $2R_g$ of PVAc40K ($R_g \sim 5.7$ nm).

by high monomer reactivity [42]. To evaluate the effect of polydispersity, we studied PNC based on monodisperse P2VP. Analysis revealed the same decrease of the interfacial effects with an increase in MW (Fig. S6 in the Supplemental Material [33]). Therefore, we treat the polydispersity as a secondary effect in the following discussions.

The revealed molecular weight dependence of the interfacial layer thickness is in stark contrast to what has been anticipated from theories [8–12] and to what can be expected from supported thin polymer film studies [20]. We see two possible reasons for this unexpected behavior: (i) PNCs require long annealing time to reach equilibrium [43,44]; or (ii) the polymer chains experience a strong frustration in chain packing in the interfacial region due to the formation of large loops at higher MW. Recent studies of supported thin polymer films revealed a strong MW dependence of the equilibrium desorption times. In the case of polystyrene, the desorption time could increase from $\sim 10^7\tau_\alpha$ for chains with MW ~ 20 kg/mol to as long as $\sim 10^{12}\tau_\alpha$ for chains with MW ~ 325 kg/mol [43,44]. To verify the desorption time effect, we annealed the PVAc253K-20% at T = 160 °C ($\tau_\alpha \sim 3$ ns) for an additional 15 days ($t_{\mathrm{ann}} \sim 1.3 \times 10^6$ s). This annealing corresponds to $4 \times 10^{14}\tau_\alpha$, which by far exceeds the longest equilibration time for polystyrene thin films of a similar MW [44]. However, such strong annealing did not produce any detectable changes in the dielectric spectra or their temperature dependence (Fig. S4).

To examine the role of chain packing in the interfacial layer, we turn to detailed analyses of the SAXS data (Fig. S3). The PVAc12K-20% can be well described by the scattering on hard spheres embedded in the polymer, implying the chain packing of the interfacial layer in this low MW sample is similar to that of the bulk matrix. However, the SAXS data for the PVAc40K-20%, PVAc85K-20%, and PVAc253K-20% can only be fit by a core-shell model with the scattering length density (SLD) of the shell (the interfacial layer) significantly lower than that of the bulk matrix. This surprising result clearly implies a reduced density in the interfacial layer of PNCs with higher MWs. To further confirm this conjecture, we performed direct density measurements. The average polymer matrix density was estimated as $\bar{\rho}_{\mathrm{mat}} = (\rho_{\mathrm{PNC}} - \rho_{\mathrm{NP}}\varphi_{\mathrm{NP}})/(1-\varphi_{\mathrm{NP}})$, where ρ_{PNC} is the density of the PNC and ρ_{NP} is the density of NP. $\bar{\rho}_{\mathrm{mat}}$ was then compared to the neat polymer density, ρ_{neat} (for raw data see Table S1 in the Supplemental Material [33]). As shown in Fig. 3(c), PNC PVAc12K-20% has a slightly (~1%) higher $\bar{\rho}_{\mathrm{mat}}$ than the neat PVAc12K. However, $\bar{\rho}_{\mathrm{mat}}$ monotonically decreases with increasing MW and is significantly lower (~4%) than that of the neat PVAc253K. A crossover MW ~30 kg/mol can be found at $\bar{\rho}_{\mathrm{mat}} = \rho_{\mathrm{neat}}$. The observed ~1% increase in $\bar{\rho}_{\mathrm{mat}}$ corresponds to ~4% denser interfacial layer in PVAc12K-20%, while the ~4% decrease corresponds to an interfacial layer with ~18% lower density if the l_{int} is assumed to be 3 nm. An even larger change in density of the interfacial layer is expected assuming $l_{\mathrm{int}} \sim 2.5$ nm [Fig. 3(a)], consistent with SAXS data (Table S2). These results are consistent with recent PALS measurements that revealed an increase of density in a supported oligomeric polymer thin film [45] and an increase in free volume in high MW PNCs [16]. The reduction of the density in the PVAc/SiO_2 PNC is also confirmed by the analysis of the specific volume data published in Ref. [15]. For example, the filled diamond in Fig. 3(c) shows a lower density of the PNC in comparison with the neat polymer, both at 293 °C and 10 MPa pressure. Since the hydrostatic pressure always reduces the free volume, a larger reduction in density may be anticipated at atmospheric pressure. Furthermore, the reduction of the average matrix density is also found in P2VP/SiO_2 PNCs

(Fig. S7) with different loadings, suggesting the universality of such phenomena in high MW PNCs with attractive polymer-NP interactions. The interfacial layer thickness of P2VP/SiO_2 is slightly larger $l_{\text{int}} \sim 5$ nm [23] than in PVAc/SiO_2. This might be related to a higher rigidity of P2VP (a larger characteristic ratio C_∞), as was suggested in recent simulations [27].

Although the free-volume hole diffusion model (FVHD) [46] anticipates a lower mass density and a lower T_g at the interface, it cannot explain the MW and annealing effect observed in the current study. This anomalous dynamic effect appears to be from a complex interplay between the long chain adsorption, nanoconfinement, and bridging effects. According to the Scheutjens-Fleer theory (SFT), the interfacial segmental concentration profiles of loops, tails, and free chains vary significantly with MW. Here, we chose a hexagonal lattice model with lattice size to be the Kuhn length of PVAc ($l_k = 1.7$ nm). Following the same definitions from their original paper [8], we set $\chi_s = 1.0$ and $\chi = 0.5$ to count the segment-NP and segment-segment interactions. The root-mean-square height of loops, h_{loop}, is defined as, $h_{\text{loop}} = \sqrt{\sum_{i=1}^{M} r_i^2 \varphi_{i,l} / \sum_{i=1}^{M} \varphi_{i,l}}$, where r_i is the distance of the ith lattice layer away from the wall, $\varphi_{i,l}$ is the concentration of loop segments at the ith lattice layer, and M is the number of lattice layers. As shown in Figs. 4 and S8, in a concentrated solution or melt, low MW chains form much shorter loops with less anchoring points per chain compared to high MW PNCs. Upon solvent evaporation, the adsorbed short chains can adjust their conformations much easier than longer chains, and therefore should form a more densely packed interface when attractive polymer-NP interactions are present. However,

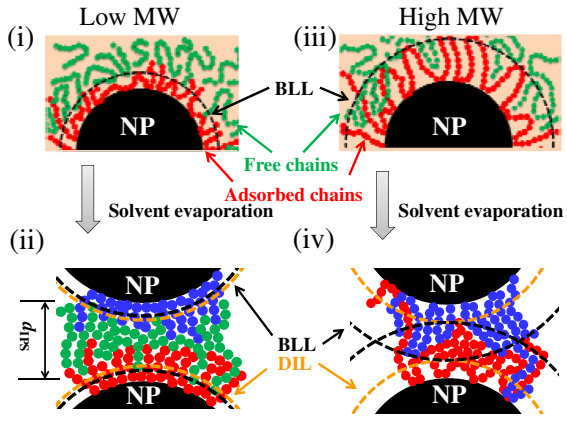

FIG. 4. The interfacial chain packing in low and high MW PNCs. The reddish brown background in (i) and (iii) denotes the solvent molecules. (i) and (iii) represent the packing of the adsorbed chain (red) and free chains (green) in solution. The black dashed lines indicate the height of loops. (ii) and (iv) represent the chain packing of low and high MW PNCs after solvent evaporation. The black lines and orange lines indicate the height of the loops and the thickness of the DIL.

long chains forming long loops and bridges between nanoparticles provide additional frustration in chain packing in PNCs. For example, d_{IPS} (~10 nm) at the loading studied is larger than $2R_g$ of PVAc12K but less than 1/2 of that of PVAc253K. Therefore, in the case of the PVAc12K-20% bridging seldom forms and there will be plenty of free (unadsorbed) chains around (Fig. 4), both of which facilitate a dense packing in the interfacial layer. However, in PVAc253K-20%, the average height of the loops, h_{loop}, is comparable to d_{IPS} [Figs. 3(a) and S8b], which leads to severe bridging between NPs, strong loop-loop repulsion, and very few free chains in this PNC. As a consequence, the packing between NPs with anchored loops will be much more like a colloidal packing, where the loops act as a screening layer and repel segments from neighboring NPs. The combination of these effects creates an interfacial layer with significant frustration in chain packing within the complex geometry of PNCs. This also explains the observed value of crossover MW [Fig. 3(c)] ~30 kg/mol, which has $2R_g \sim d_{\text{IPS}} \sim 10$ nm at the studied loading. Moreover, the onset of deviation in the dependences of density on loading also appears at $d_{\text{IPS}} \sim 2R_g$ in both PVAc40K [inset Figs. 3(c)] and P2VP100K (Fig. S7) based PNCs. These results may be in line with an earlier observation that a slowing down of the chain diffusion occurs at around $d_{\text{IPS}} \sim 2R_g$ [40].

The dependence of the interfacial layer density on molecular weight [Fig. 3(c)] provides a clear explanation for the decrease in the change of dynamics with increasing MW (Fig. 2). A more densely packed interfacial layer in low MW PNCs leads to a significant slowing down in segmental dynamics and a larger layer thickness. In contrast, the competition between the surface anchoring (enthalpic effect) and frustrated chain packing (entropic effect) causes the unexpected dynamics changes in high MW PNCs.

It is worth noting that at low MW, the DIL has slightly higher density and its thickness is similar to the h_{loop} predicted by the SFT [Fig. 3(a)], which may suggest a correlation between the static and dynamic interfacial layer thickness in equilibrium conditions, as reported for well-annealed supported thin polymer films [20]. Thus, we cannot rule out the possibility that upon long enough annealing the DIL thickness will follow the theoretical predictions for BLL even for long chains. However, according to our annealing data, to reach equilibrium in high MW PNCs might require unrealistically long times. Therefore, high MW PNCs can be considered as being trapped in a deep metastable state. Nevertheless, our results clearly emphasize the complex relationships between the DIL and BLL in terms of their MW dependencies (Fig. 4), and call for a significant revision of our understanding of equilibrium and nonequilibrium structure and dynamics in PNCs. Furthermore, the revealed dependence of the interfacial layer density on the molecular weight of PNCs provides new ways of harnessing the nonequilibrium state

[47] of soft materials at temperatures well above their glass transition temperatures, and also have strong implications on designing new materials for molecular and ion transport that might be enhanced by the additional free volume in the interfacial layer.

We thank Eric Stacy to help us set up the Fortran program. This work was supported by the U.S. Department of Energy, Office of Science, Basic Energy Sciences, Materials Sciences and Engineering Division.

S. C. and A. P. H. contributed equally to this work.

*Corresponding author.
sokolov@utk.edu

[1] S. S. Ray and M. Okamoto, Prog. Polym. Sci. **28**, 1539 (2003).
[2] C. Sanchez, B. Julian, P. Belleville, and M. Popall, J. Mater. Chem. **15**, 3559 (2005).
[3] L. S. Schadler, S. K. Kumar, B. C. Benicewicz, S. L. Lewis, and S. E. Harton, MRS Bull. **32**, 335 (2007).
[4] S. K. Kumar and R. Krishnamoorti, Annu. Rev. Chem. Biomol. Eng. **1**, 37 (2010).
[5] J. Jancar, J. F. Douglas, F. W. Starr, S. K. Kumar, P. Cassagnau, A. J. Lesser, S. S. Sternstein, and M. J. Buehler, Polymer **51**, 3321 (2010).
[6] M. E. Mackay, T. T. Dao, A. Tuteja, D. L. Ho, B. Van Horn, H. C. Kim, and C. J. Hawker, Nat. Mater. **2**, 762 (2003).
[7] P. Rittigstein, R. D. Priestley, L. J. Broadbelt, and J. M. Torkelson, Nat. Mater. **6**, 278 (2007).
[8] J. M. H. M. Scheutjens and G. J. Fleer, J. Phys. Chem. **84**, 178 (1980).
[9] P. G. De Gennes, Adv. Colloid Interface Sci. **27**, 189 (1987).
[10] O. Guiselin, Europhys. Lett. **17**, 225 (1992).
[11] A. N. Semenov, J. Bonet-Avalos, A. Johner, and J. F. Joanny, Macromolecules **29**, 2179 (1996).
[12] D. N. Theodorou, Macromolecules **21**, 1391 (1988).
[13] N. Jouault, J. F. Moll, D. Meng, K. Windsor, S. Ramcharan, C. Kearney, and S. K. Kumar, ACS Macro Lett. **2**, 371 (2013).
[14] C. J. Ellison and J. M. Torkelson, Nat. Mater. **2**, 695 (2003).
[15] R. B. Bogoslovov, C. M. Roland, A. R. Ellis, A. M. Randall, and C. G. Robertson, Macromolecules **41**, 1289 (2008).
[16] S. E. Harton, S. K. Kumar, H. Yang, T. Koga, K. Hicks, E. Lee, J. Mijovic, M. Liu, R. S. Vallery, and D. W. Gidley, Macromolecules **43**, 3415 (2010).
[17] C. Rotella, M. Wubbenhorst, and S. Napolitano, Soft Matter **7**, 5260 (2011).
[18] S. Y. Kim, H. W. Meyer, K. Saalwächter, and C. F. Zukoski, Macromolecules **45**, 4225 (2012).
[19] A. Papon, H. Montes, F. Lequeux, J. Oberdisse, K. Saalwachter, and L. Guy, Soft Matter **8**, 4090 (2012).
[20] P. Gin, N. Jiang, C. Liang, T. Taniguchi, B. Akgun, S. K. Satija, M. K. Endoh, and T. Koga, Phys. Rev. Lett. **109**, 265501 (2012).
[21] M. Füllbrandt, P. J. Purohit, and A. Schönhals, Macromolecules **46**, 4626 (2013).
[22] S. Gong, Q. Chen, J. F. Moll, S. K. Kumar, and R. H. Colby, ACS Macro Lett. **3**, 773 (2014).
[23] A. P. Holt, P. J. Griffin, V. Bocharova, A. L. Agapov, A. E. Imel, M. D. Dadmun, J. R. Sangoro, and A. P. Sokolov, Macromolecules **47**, 1837 (2014).
[24] J. Berriot, H. Montes, F. Lequeux, D. Long, and P. Sotta, Macromolecules **35**, 9756 (2002).
[25] J. Moll and S. K. Kumar, Macromolecules **45**, 1131 (2012).
[26] B. A. Pazmino Betancourt, J. F. Douglas, and F. W. Starr, Soft Matter **9**, 241 (2013).
[27] J.-M. Y. Carrillo, S. Cheng, R. Kumar, M. Goswami, A. P. Sokolov, and B. G. Sumpter, Macromolecules **48**, 4207 (2015).
[28] P. Z. Hanakata, J. F. Douglas, and F. W. Starr, Nat. Commun. **5**, 4163 (2014).
[29] T. Koga, N. Jiang, P. Gin, M. K. Endoh, S. Narayanan, L. B. Lurio, and S. K. Sinha, Phys. Rev. Lett. **107**, 225901 (2011).
[30] A. Bansal, H. C. Yang, C. Z. Li, K. W. Cho, B. C. Benicewicz, S. K. Kumar, and L. S. Schadler, Nat. Mater. **4**, 693 (2005).
[31] P. Klonos, I. Y. Sulym, K. Kyriakos, I. Vangelidis, S. Zidropoulos, D. Sternik, M. V. Borysenko, A. Kyritsis, A. Deryło-Marczewska, V. M. Gun'ko, and P. Pissis, Polymer **68**, 158 (2015).
[32] P. Klonos, A. Kyritsis, and P. Pissis, Polymer **77**, 10 (2015).
[33] See Supplemental Material at http://link.aps.org/supplemental/10.1103/PhysRevLett.116.038302, which includes Refs. [34–39]
[34] H. Kamiya, H. Suzuki, D. Kato, and G. Jimbo, J. Am. Ceram. Soc. **76**, 54 (1993).
[35] M. Iijima and H. Kamiya, Langmuir **26**, 17943 (2010).
[36] F. Kremer and A. Schohals, *Broadband Dielectric Spectroscopy* (Springer-Verlag, Berlin, 2002).
[37] P. A. M. Steeman and F. H. J. Maurer, Colloid Polym. Sci. **268**, 315 (1990).
[38] H. Schäfer, E. Sternin, R. Stannarius, M. Arndt, and F. Kremer, Phys. Rev. Lett. **76**, 2177 (1996).
[39] T. Roths, M. Marth, J. Weese, and J. Honerkamp, Comput. Phys. Commun. **139**, 279 (2001).
[40] S. Gam, J. S. Meth, S. G. Zane, C. Chi, B. A. Wood, M. E. Seitz, K. I. Winey, N. Clarke, and R. J. Composto, Macromolecules **44**, 3494 (2011).
[41] S. Cheng, S. Mirigian, J.-M. Y. Carrillo, V. Bocharova, B. G. Sumpter, K. S. Schweizer, and A. P. Sokolov, J. Chem. Phys. **143**, 194704 (2015).
[42] X. Miao, W. Zhu, Z. Zhang, W. Zhang, X. Zhu, and J. Zhu, Polym. Chem. **5**, 551 (2014).
[43] S. Napolitano and M. Wubbenhorst, Nat. Commun. **2**, 260 (2011).
[44] C. Housmans, M. Sferrazza, and S. Napolitano, Macromolecules **47**, 3390 (2014).
[45] H. J. Butt, H. Duran, W. Egger, F. Faupel, V. Harmandaris, S. Harms, K. Johnston, K. Kremer, F. Y. Lin, L. Lue, C. Ohrt, K. Raetzke, L. Ravelli, W. Steffen, and S. D. B. Vianna, Macromolecules **47**, 8459 (2014).
[46] S. Napolitano and D. Cangialosi, Macromolecules **46**, 8051 (2013).
[47] A. J. Liu, G. S. Grest, M. C. Marchetti, G. M. Grason, M. O. Robbins, G. H. Fredrickson, M. Rubinstein, and M. Olvera de la Cruz, Soft Matter **11**, 2326 (2015).